

An ASK Demodulator for Data Telemetry in Biomedical Application

Bin Liang*, Zhi Yang* and Wentai Liu

Abstract—This paper presents a demodulator design for Amplitude Shift Keying (ASK) based wireless telemetry system in biomedical application. It supports up to 300Kbits per second (bps) data rate and detects envelope with modulation index of 1% or more. The design includes a single-to-differential OTA, a current mode full-wave rectifier, a log-domain peak detector, a variable-gain amplifier and a comparator. The rising and falling time constants of our design are tunable through varying off-chip components to support a wide range of modulation indexes and data rate. The circuit blocks are designed and simulated in Taiwan Semiconductor Manufacturing Company (TSMC) 0.18 μm process and occupying 120 \times 420 μm^2 . The power consumption is 1mW with 1.8V supply voltage.

I. INTRODUCTION

Nowadays implanted electronics are becoming more and more popular and carry the hope of treatment of a wide variety of conditions – pacemakers for cardiac arrhythmia, retinal implants for the blinked [1], [2], cochlear implants for the deaf, deep-brain stimulations for Parkinson’s disease and spinal-cord stimulators for pain controlling [3]. For these applications, a data communication link between the implanted electronics and external devices is preferred, either transmitting data commands from external side to implant side to control the implanted electronics (referred to as forward data telemetry), or to transmit the diagnosed information from the implant side to external side for monitoring and/or adaptive controlling purpose (referred to as reverse telemetry) [4].

For data communication in present implanted systems, percutaneous physical links are usually not preferred because of the mismatch in material properties or scarring at the tissue interface. An alternative is a wireless inductive links, which are coupled coils forming an air core transformer. Coils are used to wirelessly deliver data through human skin, controlling the implanted electronics. Usually, wireless power transmission is also required if battery is not adopted. In Figure 1, a single band telemetry system transmitting both data and power through the same coil pair is depicted [5], [6]. This architecture advantageously reuses coil pair for both data and power, therefore, favorable to system integration and miniaturization [7], [8]. A major challenge of this approach is a sensitive data demodulator to restore signal without intervening high efficiency power transmission. A design of such data demodulator is the focus of this paper.

The rest of the paper is organized as follows. Section II describes ASK modulation scheme. Section III presents the demodulator design. Section IV shows the simulation results. Section V concludes the work.

*These authors contribute to the work equally

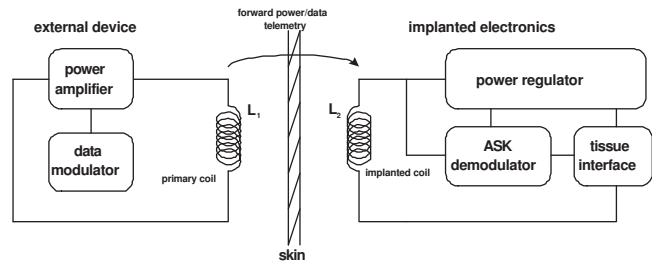


Fig. 1. Block diagram of single-band implantable system.

II. ASK MODULATION

ASK modulation scheme allows simultaneous forward power harvesting and forward data transmission through the same coil pair. Compared to recently reported telemetry designs based on dual coil pairs [3], [9], [10], the proposed architecture has two natural advantages: first, ASK based telemetry system potentially supports both high power efficiency and high data rate transmission. As shown in Figure 2, ASK spectrum includes two side bands, which carry the data signal, while the power transmission is accomplished by harvesting energy located "middle" band. With a high sensitivity demodulator, the two side bands can be designed with small energy portion, while most transmitted energy is reserved for power transmission, therefore high power efficiency can be achieved. Compared to ASK spectrum, energy of data band in phase-shift keying (PSK) and frequency-shift keying (FSK) is comparable to the power energy. In this case, power efficiency is affected and more energy needs to be delivered by the transmitter to ensure the implanted electronics can collect sufficient power. It may lead to excessive heat exposure of tissue interface.



Fig. 2. Power spectrum of different modulation scheme.

Second, coherent data demodulation method is not necessary by using ASK. Envelop detection circuit is able to well serve the data modulation. In this case, clock synchronization between implanted electronics and external electrical devices can be avoided, which dramatically simplify the implanted system.

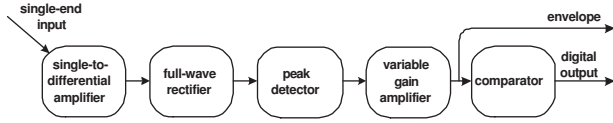


Fig. 3. Envelope Detector Block Diagram

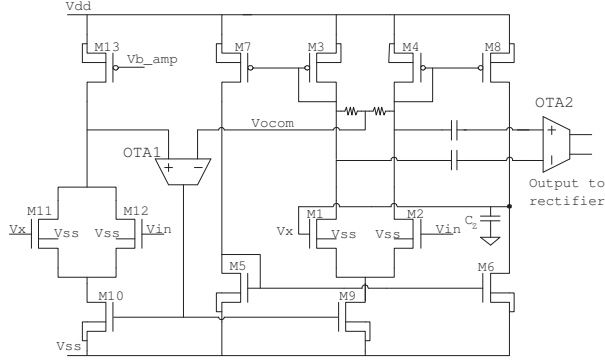


Fig. 4. Schematic of single to differential convert with feedback to suppressing tail current fluctuation.

III. ASK DEMODULATOR DESIGN

The block diagram of the ASK demodulator is shown in Figure 3.

A. Single-to-Differential Convertor

A single-to-differential amplifier is designed to convert the sensed current waveforms from implant coil to differential signals, which facilitate further full-wave rectification in current domain. As shown in Figure 4, a local feedback structure is employed (M5-M8 and C_z), which extracts the low frequency common mode fluctuation and stores on C_z . The extracted low frequency fluctuation is further applied to the non-used amplifier input (V_x in Figure 4).

Besides low frequency fluctuations, the common mode input also has frequency components within the ASK signal band, which can not be extracted and filtered by the local feedback structure (M5-M8 and C_z). Consider an ideal case that the amplifier inputs (V_{in} and V_x) are $A \sin \omega t$ and 0, respectively. The input common mode is $\frac{1}{2}A \sin \omega t$, so as the sources of input pair. Such fluctuation modulate the tail current at the frequency ω , resulting unbalanced gain during positive and negative cycles. The gain imperfections cause waveform envelope fluctuation and defect the purpose of full-wave rectification that provides two usable phases per cycle.

To maintain a constant tail current in the main amplifier, a replica of the main amplifier with scaling is used for biasing [11]. As shown in 4, the current through M10 (tail current in the replica) is forced to be a constant magnitude by the feedback OTA1. The tail current in the main amplifier is current mirrored from the replica in a cascaded fashion, therefore, less sensitive to the $\frac{1}{2}A \sin \omega t$ input common mode change.

The amplifier has one zero and two poles, which are functions of the components parameters. The zero is designed to reject low frequency common mode disturbance, while the

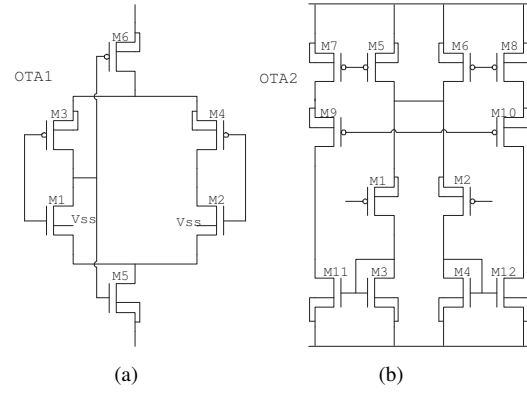


Fig. 5. a) Schematic of the OTA1 to maintain tail currents b) Schematic of the OTA2.

two poles set the passing band of the amplifier. As the first order approximation, the zero and poles are expressed as [12]

$$\omega_z = \frac{1}{(r_{d1} || r_{d2})C_z}, \quad \omega_{p1} = \frac{g_{m1}}{C_z}, \quad \omega_{p2} = \frac{g_{m3}}{C_o}, \quad (1)$$

where $r_{d1} || r_{d2}$ is the resistance seen from capacitor C_z . g_{m1} and g_{m3} are the transconductance of M_1 and M_3 , respectively.

B. Current Mode Rectifier

As show in Figure 6, a full-wave rectifier is designed based on two symmetric half-wave rectifiers [13]. I_{in1} and I_{in2} are input currents with 180 degree phase shift. When current input I_{in1} flows into node A, the voltage at node A is pulled up because of diode-connected M1a. This voltage is amplified by the M2a, fed into the gate of M3a through feedback loop formed by M4a and cut off M3a. Meanwhile, current I_{in2} flowing out of node B is mirrored to the output branch. During the next cycle, the current I_{in1} flows out of node A and it appears in the output branch instead of current I_{in2} which flows out of node B.

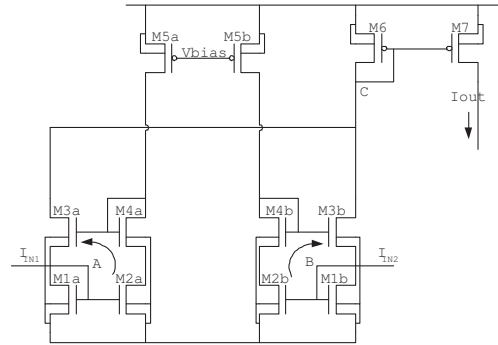


Fig. 6. Schematic of current-mode full-wave rectifier.

C. Peak Detector

The concept of log-domain current-mode peak detector was first proposed in [14] with the impressive performance of detecting waveform peaks demonstrated in [15]. As shown in Figure 7, the gate voltage of diode-connected transistor M1 is specified by the input current I_{in} . During the attacking

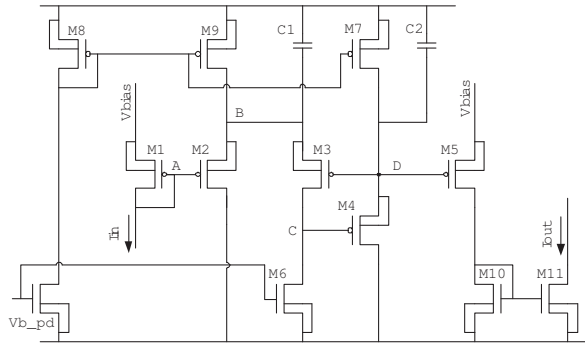


Fig. 7. Schematic of log-domain current-mode peak detector.

phase, I_{in} increases; voltage at node A decreases. Node B follows the change of node A, also decrease. Since transistor M6 will maintain the current flowing through M3, voltage at node C is pulled down, hence open transistor M4, which makes voltage at node D go down. This voltage is converted into current output. Similarly, during the release phase, I_{in} decrease; voltage at node B increases. Due to the effect of M3, transistor M4 is cut off. M7 keep charging capacitor C2 and pull up voltage of node D.

According to [15], releasing and attacking time constants are functions of circuit parameters

$$\tau_a \sim \frac{C_{sa}}{I_a}, \tau_r \sim \frac{C_{sr}}{I_r}, \quad (2)$$

where I_a and I_r are bias currents of transistors M6 and M7, respectively. By varying the I_a , I_b , C_{sa} and C_{sr} , the attacking and releasing time constants are tunable to accommodate a wide frequency range. In this design, I_a , I_b and C_{sa} are chosen as $300nA$, $1\mu A$, $1pf$; C_{sr} is off-chip component, defaulted at $125pf$.

D. Variable Gain Amplifier and Comparator

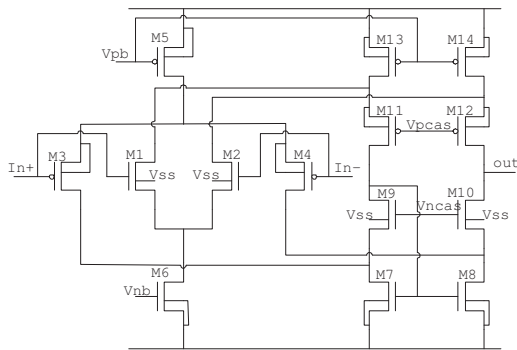


Fig. 8. Self-bias differential cascaded OTA used to built the band pass filter.

The detected waveform envelope by the peak detector is bandpass filtered and amplified through a first order filter built from the self-bias differential OTA (Figure 8). The filtering process is important, as the detected envelope contains very low frequency modulation due to coil coupling variation as well as $4MHz$ ripples that is caused by the finite

releasing constant of the peak detector. Increase the releasing time constant of the peak detector can reduce the $4MHz$ ripples, however, limited the symbol interval and data rate.

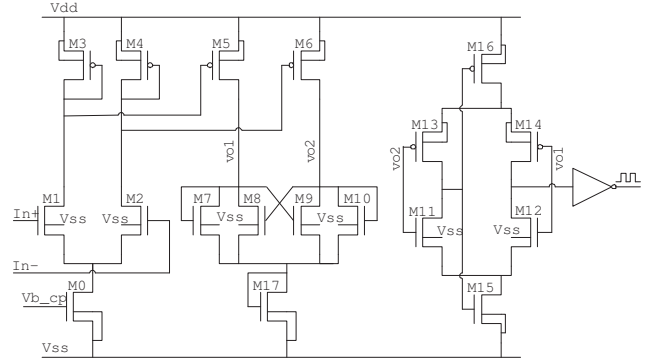


Fig. 9. Comparator(need modification).

The comparator shown in (Figure 9) is included at the end. This design is adopted form [15].

IV. SIMULATION RESULTS

The ASK demodulator is designed and simulated in TSMC $.18\mu m$ CMOS technology. The layout of the demodulator is shown in Figure 10. The total power power consumption is simulated to be $1mW$, among which more than 50% is consumed by the transconductance amplifier (OTA2) to accommodate a relative wide range input signal magnitude.

The simulation results of 5% modulation index with $100KHz$ data rate is shown in Figure 11. By replacing the storing capacitor of the peak detector, the detection time constants can be tuned to support other data rate. As shown in Figure 12, the simulation of results of 1% modulation index with $50KHz$ data rate is plotted.

V. CONCLUSION

An ASK demodulator designed is presented to fulfill data communication in biomedical application. The circuits senses ASK current signal from the implant coil as input, and output analog waveform envelope as well as digitalized "1" and "0" bits streams. The rising and falling time constants of the envelope detector are tunable by using off-chip capacitors. Therefore, it can support a wide range of modulation indexes and data rates. The circuits consumes total power of $1mW$ at $1.8V$ supply voltage and the layout area is $120 \times 420\mu m^2$.

REFERENCES

- [1] W. Liu, K. Vichienchom, M. Clements, S. DeMarco, C. Hughes, E. McGucken, M. Humayun, E. De Juan, J. Weiland, and R. Greenberg, "A neuro-stimulus chip with telemetry unit for retinal prosthetic device," *IEEE Journal of Solid-State Circuits*, vol. 35, no. 10, pp. 1487–1497, Oct 2000.
- [2] M. Ortmanns, N. Unger, A. Rocke, M. Gehrke, and H. Tietdke, "A $01mm^2$ digitally programmable nerve stimulation pad cell with high-voltage capability for a retinal implant," in *ISSCC Dig. of Tech. Papers*, Feb 2006, pp. 89–98.
- [3] M. Baker and R. Sarpeshkar, "Feedback analysis and design of rf power links for low-power bionic systems," *IEEE Transactions on Biomedical Circuits and System*, vol. 1, no. 1, pp. 28–38, March 2007.

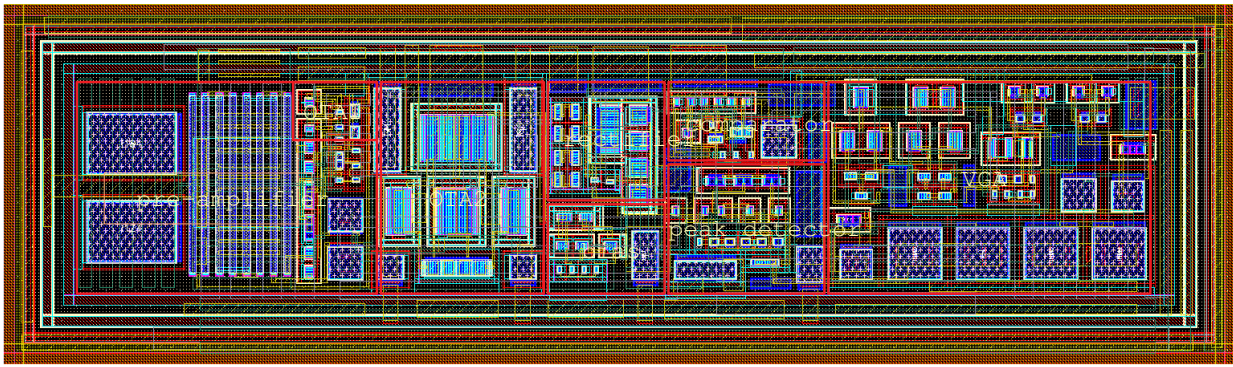


Fig. 10. layout of the envelope detector.

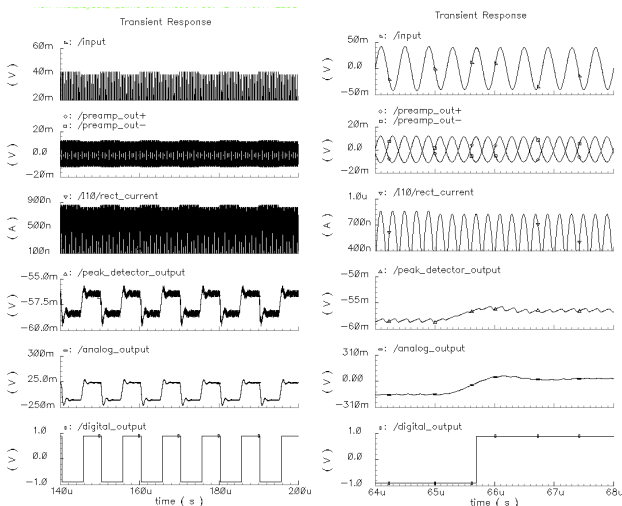


Fig. 11. Simulation of envelope detector with modulation depth set to be 5%. The data rate is 100KHz. Left part: the first trace is the modulated waveforms from the class-E amplifier; the second trace is the differential voltage generated by the single-to-differential converter; the third trace is the output of current mode rectifier; the fourth trace is the output of peak detector; the fifth trace is the analog waveform envelope output; the sixth trace is the digital output. Right part is the zoom in view of traces in the left part.

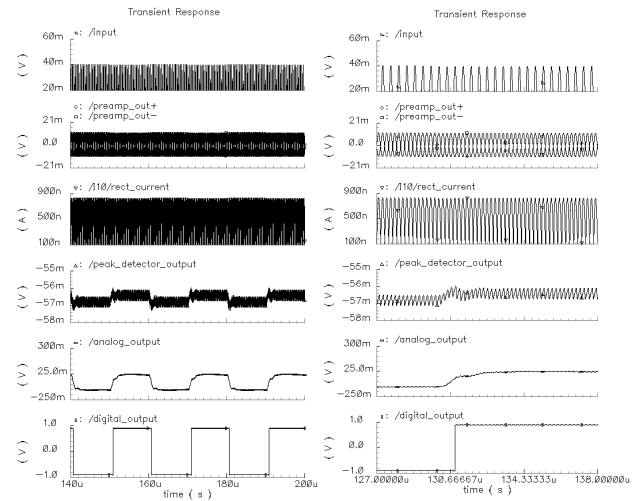


Fig. 12. Simulation of envelope detector with modulation depth set to be 1%. The data rate is 50KHz. Left part: the first trace is the modulated waveforms from the class-E amplifier; the second trace is the differential voltage generated the single-to-differential converter; the third trace is the output of current mode rectifier; the fourth trace is the output of peak detector; the fifth trace is the analog waveform envelope output; the sixth trace is the digital output. Right part is the zoom in view of traces in the left part.

[4] Z. Tang, B. Smith, J. Schild, and P. Peckham, "Data transmission from an implantable biotelemetry by load-shiftkeying using circuit configuration modulator," *IEEE Transactions on Biomedical Engineering*, vol. 42, no. 5, pp. 424–428, May 1995.

[5] C. Sauer, M. Stanacevic, G. Cauwenberghs, and N. Thakor, "Power harvesting and telemetry in cmos for implanted devices," *IEEE Transactions on Circuits and Systems I*, vol. 52, no. 12, pp. 2605–2613, December 2005.

[6] Z. Hamici, R. Itti, and J. Champier, "A high-efficiency power and data transmission system for biomedical implanted electronic devices," *Measurement Science and Technology*, vol. 7, no. 2, pp. 192–201, February 1996.

[7] G. Kendir, W. Liu, W. G., M. Sivaprakasam, R. Bashirullah, M. Humayun, and J. Weiland, "An optimal design methodology for inductive power link with class-e amplifier," *IEEE Trans. Circ. and Syst. I*, vol. 52, no. 5, pp. 857–866, May 2005.

[8] Z. Yang, W. Liu, and E. Basham, "Inductor modeling in wireless links for implantable electronics," *IEEE Trans. Magn.*, vol. 43, no. 10, pp. 3851–3860, Oct 2007.

[9] M. Zhou and W. Liu, "A non-coherent psk receiver with interference cancellation for transcutaneous neural implant," in *ISSCC Dig. of Tech. Papers*, Feb 2007, pp. 156–157.

[10] M. Ghovanloo and N. K., "A high-rate frequency shift keying de-

modulator chip for wireless biomedical implants," *IEEE Proceedings, Circuits and Systems, ISCAS*, vol. 5, no. 5, pp. 25–28, May 2003.

[11] K. Gulati and H. Lee, "A high-swing cmos telescopic operational amplifier," *IEEE Journal of Solid State Circuits*, vol. 33, no. 12, pp. 2010–2019, Dec 1998.

[12] G. Palmisano and S. Pennisi, "Cmos single-input differential-output amplifier cells," *Circuits, Devices and Systems, IEE Proceedings*, vol. 150, no. 3, pp. 194–198, Jun 2003.

[13] S. Khucharoensin and V. Kasemsuwan, "A high performance cmos current-mode precision full-wave rectifier," *Circuits and Systems, Proceedings of the 2003 International Symposium on*, vol. 1, 2003.

[14] D. Frey, "Log-domain filtering: An approach to current-mode filtering," *Proc. Inst. Electr. Eng.*, vol. 140, 1993.

[15] S. Zhak, M. Baker, and R. Sarpeshkar, "A low-power wide dynamic range envelope detector," *IEEE Journal of Solid State Circuits*, vol. 38, no. 10, pp. 1750–1753, Oct 2003.